

Electronic Supplementary Information

Probing the charging mechanisms of carbon nanomaterial polyelectrolytes

Stephen A. Hodge, Hui Huang Tay, David B. Anthony, Robert Menzel, David J. Buckley, Patrick L. Cullen, Neal T. Skipper, Christopher A. Howard, and Milo S. P. Shaffer

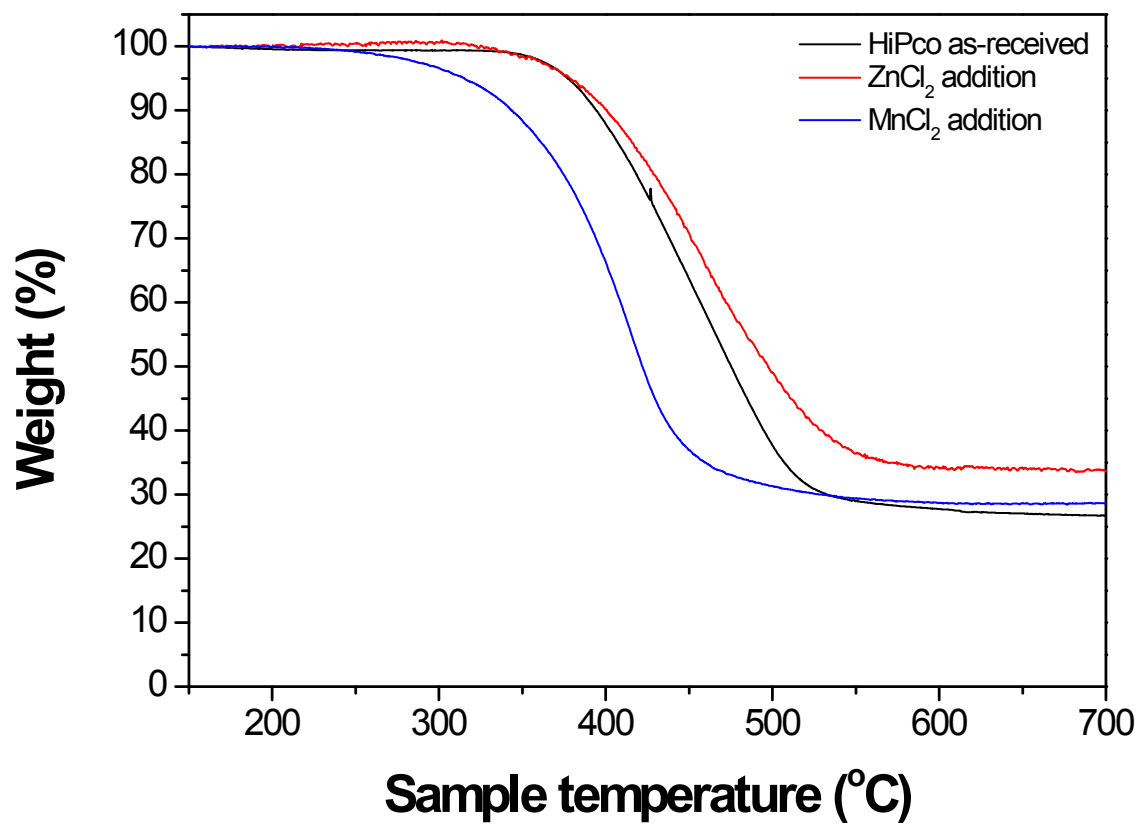


Fig. S1 Oxidative thermogravimetric analysis (TGA) of raw HiPco SWCNTs and sodium nanotubide (NaC₁₀) dispersions following reaction with manganese and zinc chloride salts.

Table S1 TGA and ICP-AES results for graphenide (KC_8 and KC_{24}) reactions with metal salts/complexes

M (compound)	Reaction stoichiometry	TGA data			ICP-AES data			M:C molar ratio
		Carbon mass	Carbon molar quantity	Residue mass	M in 100 mL 10% HCl	M mass in residue	M molar quantity	
	M:K	mg	mol	mg	mg/L	mg	mol	C/M
KC_8 reactions								
Mn (MnCl₂)	0.5:1	0.77157	6.42×10^{-5}	0.17341	0.076	0.0076	1.38×10^{-7}	464.3635
Zn (ZnCl₂)	0.5:1	0.69236	5.76×10^{-5}	0.15989	0.351	0.0351	5.37×10^{-7}	107.3716
Zn (ZnCl₂)	3:1	0.89250	7.43×10^{-5}	0.19643	0.528	0.0528	8.08×10^{-7}	92.0114
Zn (ZnCl₂)	10:1	0.93699	7.80×10^{-5}	0.15494	0.581	0.0581	8.89×10^{-7}	87.7859
Cu (CuCl₂)	0.5:1	1.50930	1.26×10^{-4}	0.22781	0.090	0.0090	1.42×10^{-7}	887.2397
Cu (CuMes)	1:1	0.33752	2.81×10^{-5}	0.40138	1.753	0.17532	2.76×10^{-6}	10.1854
KC_{24} reactions								
Mn (MnCl₂)	0.5:1	0.45004	3.75×10^{-5}	0.10301	0	0	0	--
Zn (ZnCl₂)	0.5:1	1.07776	8.97×10^{-5}	0.16023	0.12	0.012	1.84×10^{-7}	488.8862

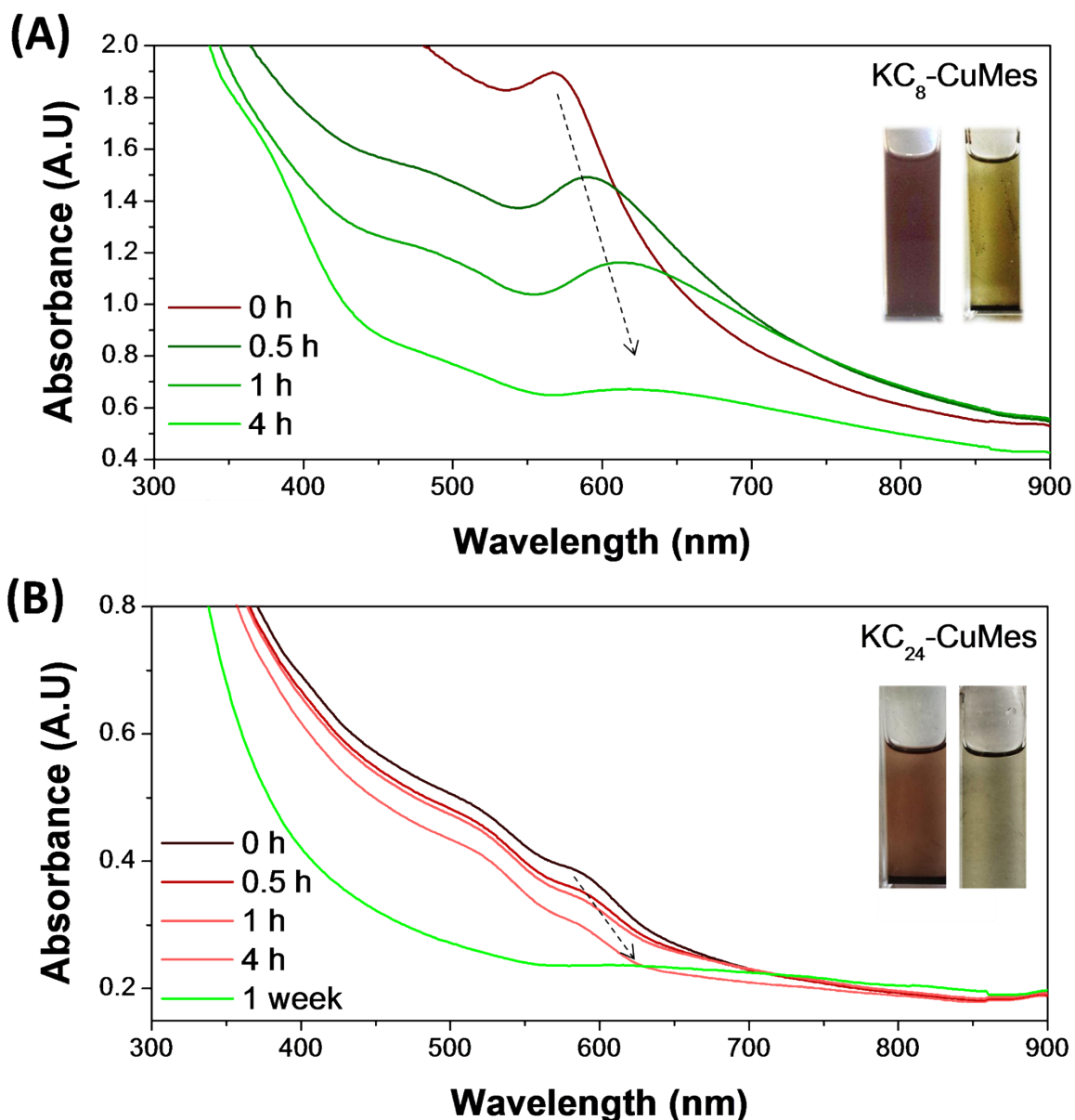


Fig. S2 UV-vis absorption spectra for Cu NPs generated by the reduction of CuMes by (A) KC_8 and (B) KC_{24} after exposure to air. The Cu metal plasmon at 570 nm is visible in both spectra. The reduction in absorption intensity over time is due to the sedimentation of graphene particles. Upon exposure to air there is a surface plasmon shift for the KC_8 generated Cu NPs due to rapid oxidation, also observed by a solution colour change from red to green. The KC_{24} generated Cu NPs were highly stable to oxidation with no shift of the surface plasmon. Typically, the solubility of these NPs is aided by adding stabilising alkylamine ligands or surfactants;¹ in the present case no additional ligands or surfactants were added suggesting stabilisation may be provided to some extent by the amidic solvent. Further UV-vis and TEM investigations are required to ascertain the stabilising mechanism of the KC_{24} generated Cu NPs.

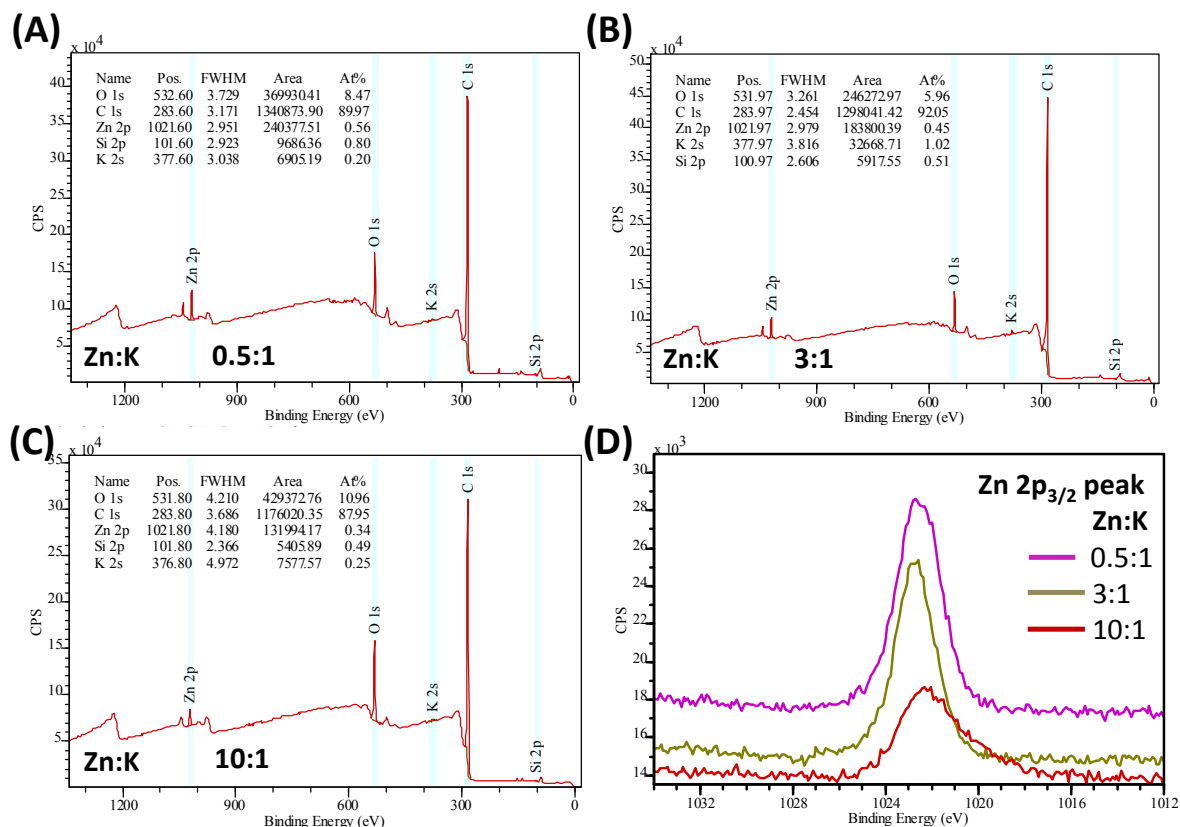


Fig. S3 XPS survey spectra (A)-(C) for KC_8 samples following reaction with ZnCl_2 with varying $\text{Zn}^{2+}:\text{K}$ stoichiometry. (D) High resolution scan of the $\text{Zn } 2p_{3/2}$ region for the products (A)-(C).

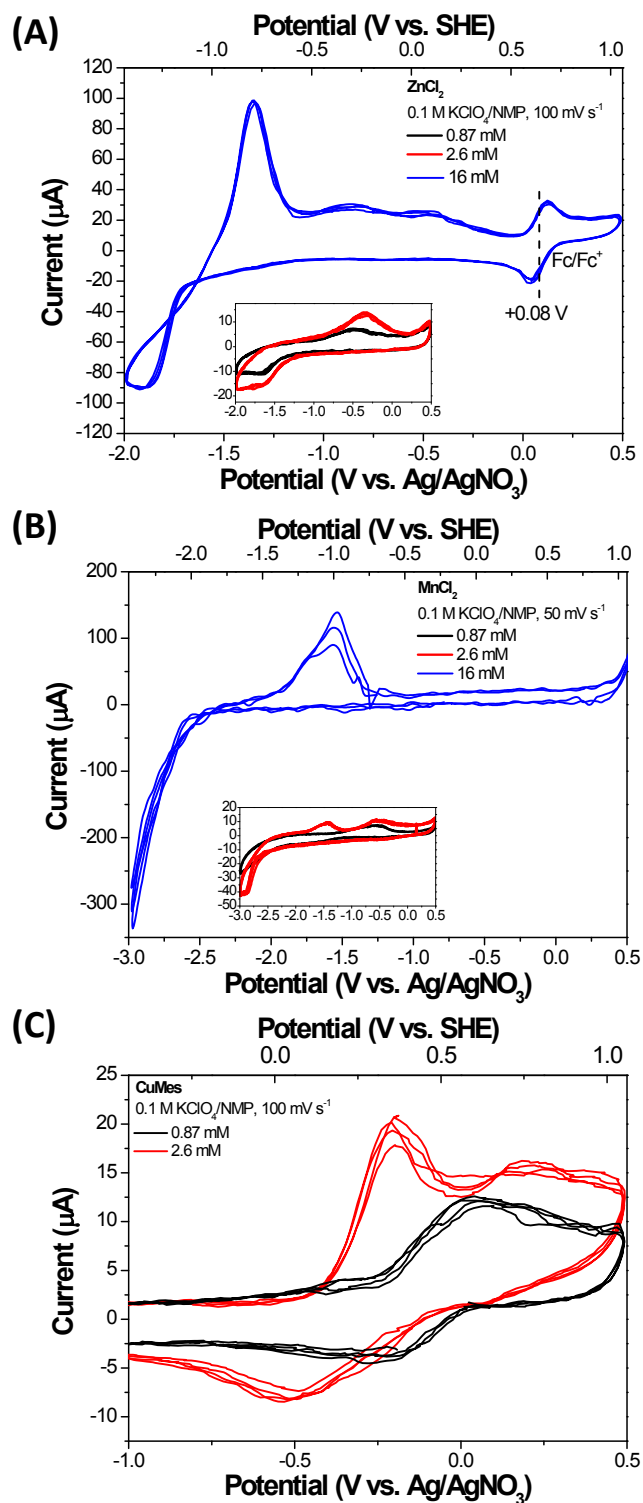


Fig. S4 CV at a platinum working electrode of the metal salts/complexes used in this study in non-aqueous electrolyte (0.1 M KClO₄/NMP). (A) 16 mM ZnCl₂ CV showing the Fc/Fc⁺ reference; inset shows the redox activity at lower ZnCl₂ concentrations. (B) 16 mM MnCl₂ CV; inset shows the redox activity at lower MnCl₂ concentrations. (C) CuMes CV at 0.87 mM and 2.6 mM concentrations.

Derivation of metal salt/complex reduction potentials

At low metal concentrations (0.87 mM / 2.6 mM typical of KC_{24} and KC_8 reactions, respectively, where $\text{Zn}^{2+}:\text{K}$ is 0:5:1), Nernstian behaviour is observed for the ZnCl_2 with a redox potential ~ -1.06 V *vs.* Ag/AgNO_3 (-0.50 V *vs.* SHE), however, at 16 mM ($\text{Zn}^{2+}:\text{K}$, 3:1 reaction), the voltammogram displays significant cathodic current due to zinc deposition² with an onset of ~ -1.69 V *vs.* Ag/AgNO_3 (-1.13 V *vs.* SHE). For MnCl_2 (Fig. S3B), it is difficult to determine the cathodic peak potential at 16 mM concentration, although the onset potential can be deduced as -2.57 V *vs.* Ag/AgNO_3 (-2.01 V *vs.* SHE). CuMes voltammograms (Fig. S3C) showed distinct redox features centred ~ -0.12 V *vs.* Ag/AgNO_3 ($+0.44$ V *vs.* SHE).

References

1. C. Barriere, K. Piettre, V. Latour, O. Margeat, C.-O. Turrin, B. Chaudret and P. Fau, *J. Mater. Chem.*, 2012, **22**, 2279-2285.
2. Y. Yao, S. L. Xu, Y. Xia, Y. C. Yang, J. Liu, Z. L. Li and W. Huang, *Int. J. Electrochem. Sci.*, 2012, **7**, 3265-3273.